

Cite this: *Chem. Commun.*, 2011, **47**, 3454–3456

www.rsc.org/chemcomm

COMMUNICATION

Novel C_3 -symmetric n-type tris(aroyleneimidazole) and its analogs: synthesis, physical properties and self-assembly†David Hanifi,^{ab} Dennis Cao,^{‡a} Liana M. Klivansky^a and Yi Liu^{*a}

Received 2nd November 2010, Accepted 15th January 2011

DOI: 10.1039/c0cc04753h

Novel n-type C_3 -symmetric materials are synthesized and shown to have desirable bandgap, broad absorption and high thermal stability, thus pose as viable candidates for organic photovoltaics. The strong intermolecular interactions among the extended π -surfaces beget the self-assembly of nanofibers.

Discotic molecules have emerged¹ as a new generation of organic semiconductors that have found applications in organic photovoltaics (OPVs),² organic light emitting diodes (OLEDs),³ and organic field effect transistors (OFETs).⁴ Such molecules contain polycyclic aromatic cores that have the propensity to stack into parallel-aligned columns with high charge-carrier mobilities in the mesophase, while flexible side chains are often present to ensure solubility and self-healing properties. For advanced electronic applications, both p-type (hole conducting) and n-type (electron conducting) semiconductors are required for the fabrication of complementary logic circuits⁵ or for use as active layer materials in OPVs and OLEDs.⁶ Many p-type molecules with mobilities comparable to or surpassing that of amorphous silicon have been synthesized in the past few decades, including triphenylenes,⁷ phthalocyanines,⁸ porphyrins,⁹ hexabenzocoronene,¹⁰ and truxenes.¹¹ Conversely, n-type molecular systems with desirable physical properties are currently very limited.¹² We are particularly interested in developing n-type materials for OPV applications, which require not only good electron mobility, but also (1) good light absorptivity in the visible and near infrared regions, (2) high thermal and chemical stability, (3) a properly engineered bandgap to match complementary p-type materials and the work function of the cathodes, and (4) controllable self-organization to give bicontinuous nanophase segregation in thin films for efficient charge separation and charge collection.

A good strategy for introducing n-type characteristics into a molecule is to incorporate electron-withdrawing π systems into

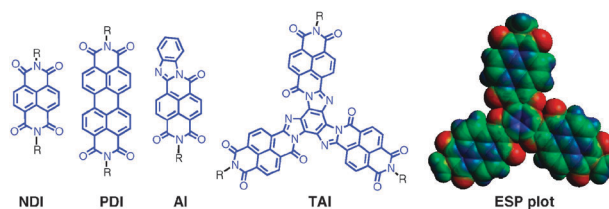


Fig. 1 Molecular structures of NDI, PDI, AI and the designed TAI. The ESP plot of TAI (R = Me) is also shown.

the aromatic core to decrease the energy level of the lowest unoccupied molecular orbital (LUMO). Imide-substituted aryls, such as naphthalene diimide¹³ (NDI) and perylene diimide¹⁴ (PDI) derivatives, are known as high performance n-type semiconductors (Fig. 1). Structurally similar aroylene imidazole¹⁵ (AI) derivatives, commonly employed in the pigment industry due to their high absorptivity and excellent thermal stability, have not been explored as n-type molecules until very recently.¹⁶ By incorporation of the AI units, a new library of versatile n-type molecules has been created. A planar C_3 -symmetrical core containing three fused AI units, namely tris(aroylene imidazole) (TAI), was designed (Fig. 1) to have enhanced n-type characteristics and optical properties due to extended delocalization of π electrons. Molecular modeling has confirmed¹⁷ the planar and electron deficient nature of the core, as indicated by a high electron affinity (LUMO energy: -3.7 eV) and by the electrostatic potential (ESP) plot, which shows delocalized negative charges. The computed energy of the highest occupied molecular orbital (HOMO) is -6.3 eV, commensurate with a bandgap of 2.6 eV.

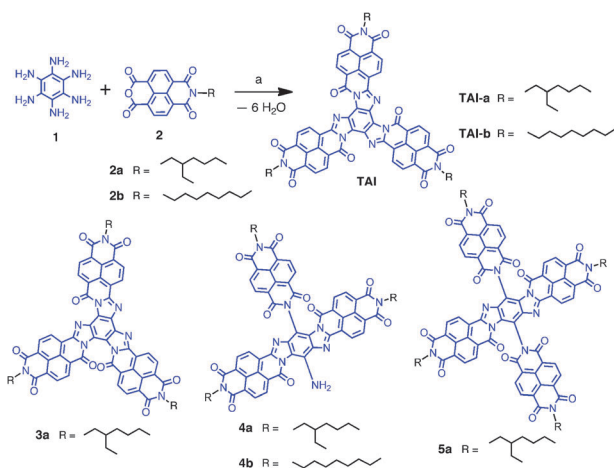
The synthesis of TAI was first attempted (Scheme 1) by heating a mixture of hexaaminobenzene (**1**)¹⁸ and mono-anhydride **2a**¹⁹ in DMF in the presence of $Zn(OAc)_2$. Orange, green and deep red fractions were isolated from this reaction. Mass spectrometry (MS) revealed (see ESI†) molecular ion peaks at m/z 1577.6, 1216.3 and 1198.3. These peaks indicate the formation of a tetra-adduct after the loss of six equiv. of H_2O , and tri-adducts after the loss of five and six equiv. of H_2O , respectively. ¹H NMR spectra of the orange and the green adducts show well-resolved resonances (see ESI†) in the aromatic region, assignable to the C_2 -symmetric tetramer **5a** and the acyclic trimer **4a**, respectively. In contrast, the ¹H NMR spectrum of the red tri-adduct is (Fig. 2c) very

^a The Molecular Foundry, Lawrence Berkeley National Laboratory, Berkeley, California 94720, USA. E-mail: yliu@lbl.gov; Fax: +1 510-486-7413; Tel: +1 510-486-6287

^b University of California, Berkeley, USA

† Electronic supplementary information (ESI) available: Synthetic details and full characterization data of the new compounds. Details of molecular modeling, thermal analysis and electrochemical analysis. UV-vis spectra of thin films and fluorescence spectra. Powder XRD plot of TAI-b. See DOI: 10.1039/c0cc04753h

‡ Current address: Chemistry Department, Northwestern University, Evanston, IL, USA.



Scheme 1 The condensation reaction that leads to the formation of different products. Solvent: dimethylformamide (DMF) or quinoline.

broad at room temperature, suggesting strong aggregation in solution. When heated at 100 °C in $\text{C}_6\text{D}_5\text{Cl}$, the broad resonances in the aromatic region split (Fig. 2d) into multiple doublets, corresponding to an unsymmetrical species. Since MS suggests the formation of a cyclic trimer, the red fraction can be readily identified as **3a**. Surprisingly, the symmetrical **TAI-a** was not observed. The condensation reaction was then carried out under different conditions. A substoichiometric amount of monoanhydride **2b** was added slowly into the solution of **1** and $\text{Zn}(\text{OAc})_2$ in quinoline over 1 hour and the mixture was kept at 170 °C for 18 hours. Aside from a trace amount of tetra-adduct, two major fractions, one green and the other deep red, were isolated using recycling size exclusion chromatography. As in the case of **4a**, the green product was identified as acyclic trimer **4b** according to MS and ^1H NMR

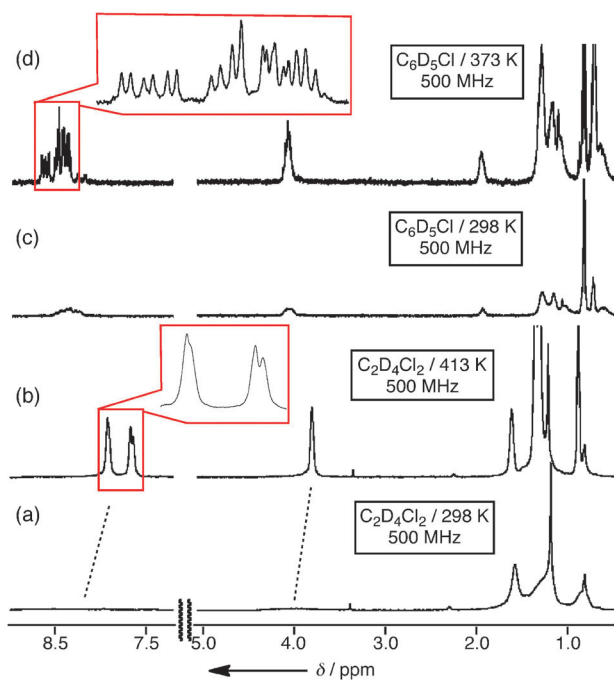


Fig. 2 ^1H NMR spectra of **TAI-b** at (a) 298 K and (b) 413 K in $\text{C}_2\text{D}_2\text{Cl}_2$ (8.0 mM), and of **3a** at (c) 298 K and (d) 373 K in $\text{C}_6\text{D}_5\text{Cl}$ (1.6 mM). The insets are the blow-up of the aromatic resonances.

spectroscopy. The red product **TAI-b** has the same mass as **3a** and can be assigned to be a cyclic trimer. The ^1H NMR spectrum of **TAI-b** in $\text{C}_2\text{D}_2\text{Cl}_2$ solution is again very broad at room temperature due to strong aggregation (Fig. 2a). In sharp contrast to **3a**, the high temperature ^1H NMR spectrum at 140 °C indicates its symmetrical nature, as evidenced by the presence of only two well-defined resonances in the aromatic region. The high symmetry of **TAI-b** is also confirmed by its ^{13}C NMR spectrum (see ESI †). In addition, all the compounds are shown to have high thermal stability by thermogravimetric analysis (see ESI †); **TAI-b** has the highest thermal stability with an onset decomposition temperature of 462 °C.

The absorption (Fig. 3a) and emission spectra (see ESI †) of these compounds were measured both in solution and in the thin film. The UV-vis spectrum of an alkyl substitute monomeric **AI** ($R = n\text{-C}_8\text{H}_{17}$) is also recorded for comparison, with an absorption maximum at 446 nm assignable to $n\text{-}\pi^*$ transition. As expected, both **TAI-b** and **3a** have an absorption band that is red shifted around 30 nm with respect to that of **AI**. The tetramer **5a** has three absorption shoulders at 460 nm, 485 nm and 520 nm. In comparison, the acyclic trimer **4b** has a distinct absorption centered at 615 nm, probably resulting from intramolecular charge-transfer between the aniline and the **AI** unit. All the solid-state UV-vis spectra show (see ESI †) a bathochromic red shift (*ca.* 10 nm) compared to solution spectra, suggesting greater structural organization in the solid state. The extinction coefficients and optical bandgaps derived from the onset of the compounds long wavelength absorption spectra are listed in Table 1. **TAI-b**, **3a** and **5a** have similar values of around 2.2 eV, while **4b** has a lower optical bandgap around 1.7 eV.

The electrochemical properties of these **AI** derivatives were investigated by cyclic voltammetry (CV) in dry CH_2Cl_2 , using the ferrocene/ferrocenium (F_c/F_c^+) redox couple as the internal standard. All the compounds undergo multiple reversible or pseudo-reversible reductions upon cathodic scan (see ESI †). No oxidation waves are observed during anodic scan except for those of the acyclic trimers. Each imide subunit of these molecules can accept two electrons, with the tetramer **5a** being a remarkable eight-electron acceptor. The CVs of both **TAI-b** and **3a** have three pseudo-reversible reduction waves. Respective LUMO energies are determined²⁰ to be -3.7 eV and -3.6 eV (Table 1), which agree very well with the modeling result. Five stepwise reduction processes are clearly identified in the CV of the tetramer **5a**, indicative of the presence of distinctive radical anion species and strong

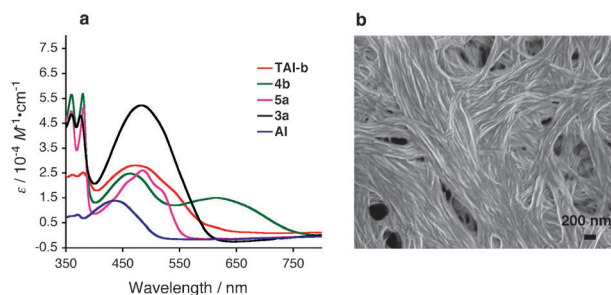


Fig. 3 (a) Solution UV-vis spectra (CH_2Cl_2 , 10.0 μM) of **TAI-b**, **3a**, **4b**, **5a** and the monomeric **AI**. (b) SEM image of nanofibers of **TAI-b**.

Table 1 Optical and electrochemical properties of the AI derivatives

Compd.	$\lambda_{\text{abs}}^{a,b}/\text{nm}$	$\epsilon/\text{M}^{-1}\text{cm}^{-1}$	E_g^c/eV	LUMO/eV	HOMO/eV
TAI-b	472 (483)	28 000	2.1	-3.7	-5.8
3a	479 (490)	52 100	2.0	-3.6	-5.6
4b	615 (620)	15 000	1.7	-3.8	-5.5
5a	515 (520)	18 200	2.3	-3.8	-6.1

^a From solutions in CH_2Cl_2 . ^b The data in parentheses are recorded from thin film. ^c Optical bandgap.

electron-accepting ability. CV of the acyclic trimer **4b** shows not only well-resolved reduction peaks, but also the presence of an anodic peak that corresponds to oxidation of its aniline moiety. The derived bandgap is 1.7 eV and is in good agreement with the optical bandgap (1.7 eV) estimated from the UV-vis spectrum.

The extended conjugation in **TAI-b** promotes strong π - π intermolecular interactions. Supramolecular aggregation of **TAI-b** is observed in solution, as indicated by the broad ¹H NMR resonances of aromatic protons and the methylene protons next to the imide unit. As a result, a phase-separated precipitate is formed from its CHCl_3 solution within one day upon standing at room temperature. Scanning electron microscopy (SEM) indicates (Fig. 3b) the formation of highly entangled nanofibers, while the birefringence from polarized optical microscopy strongly suggests anisotropic stacking (see ESI†). Powder X-ray diffraction reveals *d*-spacings of 21.4 Å and 3.9 Å, attributable to **TAI-b** column formation and slipped π - π cofacial stacking,^{14b} respectively (see ESI†). The lack of phase transitions up to 350 °C by differential scanning calorimetry (see ESI†) suggests that **TAI-b** remains crystalline at high temperature.

In summary, n-type molecules with a novel C_3 -symmetric aromatic core were designed, synthesized, and characterized. They were shown to have high thermal stability, desirable bandgap and broad absorption in the visible range. The extended large π -surface in the symmetric **TAI-b** ensures strong intermolecular interactions, promoting nanofiber assembly. The novel molecular skeleton invites future design and synthesis of new n-channel semiconductors. Its ready self-assembly of 1D nanostructures may broaden the scope of nano- and microscale organic semiconductors, and also sets the stage for sensing applications.²¹

This work was performed at the Molecular Foundry, Lawrence Berkeley National Laboratory, and was supported by the Office of Science, Office of Basic Energy Sciences, of the U. S. Department of Energy under contract No. DE-AC02-05 CH11231.

Notes and references

- (a) S. Laschat, A. Baro, N. Steinke, F. Giesselmann, C. Hagele, G. Scalia, R. Judele, E. Kapatsina, S. Sauer, A. Schreivogel and M. Tosoni, *Angew. Chem., Int. Ed.*, 2007, **46**, 4832; (b) S. Sergeev, W. Pisula and Y. H. Geerts, *Chem. Soc. Rev.*, 2007, **36**, 1902; (c) T. Kato, T. Yasuda, Y. Kamikawa and M. Yoshio, *Chem. Commun.*, 2009, 729.
- (a) L. Schmidt-Mende, A. Fichtenkotter, K. Müllen, E. Moons, R. H. Friend and J. D. Mackenzie, *Science*, 2001, **293**, 1119; (b) W. Wong, D. J. Jones, C. Yan, S. E. Watkins, S. King, S. A. Haque, X. Wen, K. P. Ghiggino and A. B. Holmes, *Org. Lett.*, 2009, **11**, 975; (c) W. Wallace, H. Wong, T. B. Singh, D. Vak, W. Pisula, C. Yan, X. Feng, E. L. Williams, K. L. Leok, Q. Mao,

- D. J. Jones, C.-Q. Ma, K. Müllen, P. Bäuerle and A. B. Holmes, *Adv. Funct. Mater.*, 2010, **20**, 927.
- (a) I. Seguy, P. Jolinat, P. Destruel, J. Farenc, R. Mamy, H. Bock, J. Ip and T. P. J. Nguyen, *J. Appl. Phys.*, 2001, **89**, 5442; (b) T. Hassheider, S. A. Benning, H.-S. Kitzerow, M.-F. Achard and H. Bock, *Angew. Chem., Int. Ed.*, 2001, **40**, 2060.
- (a) I. O. Shklyarevskiy, P. Jonkheijm, N. Stutzmann, D. Wasserberg, H. Wondergem and P. C. M. Christianen, *J. Am. Chem. Soc.*, 2005, **127**, 16233; (b) W. Pisula, Z. Tomovic, M. Stepputat, U. Kolb, T. Pakula and K. Müllen, *Chem. Mater.*, 2005, **17**, 2641.
- H. Klauk, U. Zschieschang, J. Pflaum and M. Halik, *Nature*, 2007, **445**, 745.
- (a) J.-L. Bredas, J. E. Norton, J. Cornil and V. Coropceanu, *Acc. Chem. Res.*, 2009, **42**, 1691; (b) J. Peet, A. J. Heeger and G. C. Bazan, *Acc. Chem. Res.*, 2009, **42**, 1700.
- (a) S. Kumar, *Liq. Cryst.*, 2004, **31**, 1037; (b) A. A. O. Sarhan and C. Bolm, *Chem. Soc. Rev.*, 2009, **38**, 2730.
- (a) D. Atilla, N. Kilinc, F. Yuksel, A. G. Gurek, Z. Z. Ozturk and V. Ahsen, *Synth. Met.*, 2009, **159**, 13; (b) Y. Zhang, H. Dong, Q. Tang, S. Ferdous, F. Liu, S. C. B. Mannsfeld, W. Hu and A. L. Briseno, *J. Am. Chem. Soc.*, 2010, **132**, 11580.
- (a) Q. Sun, L. Dai, X. Zhou, L. Li and Q. Li, *Appl. Phys. Lett.*, 2007, **91**, 253505; (b) X. Zhou, S. Kang, S. Kumar, S. Cheng and Q. Li, *Chem. Mater.*, 2008, **20**, 3551.
- (a) J.-S. Wu, M. D. Watson, L. Zhang, Z.-H. Wang and K. Müllen, *J. Am. Chem. Soc.*, 2004, **126**, 177; (b) W. Pisula, M. Kastler, D. Wasserfallen, T. Pakula and K. Müllen, *J. Am. Chem. Soc.*, 2004, **126**, 8074; (c) Z.-H. Wang, M. D. Watson, J.-S. Wu and K. Müllen, *Chem. Commun.*, 2004, 336; (d) J.-S. Wu, W. Pisula and K. Müllen, *Chem. Rev.*, 2007, **107**, 718.
- (a) J. Luo, Y. Zhou, Z.-Q. Niu, Q.-F. Zhou, Y. Ma and J. Pei, *J. Am. Chem. Soc.*, 2007, **129**, 11314; (b) B. Zhao, B. Liu, R. Q. Png, K. Zhang, K. A. Lim, J. Luo, J. Shao, P. K. H. Ho, C. Chi and J.-S. Wu, *Chem. Mater.*, 2010, **22**, 435.
- (a) K. A. McMenimen and D. G. Hamilton, *J. Am. Chem. Soc.*, 2001, **123**, 6453; (b) K. Pieterse, P. A. van Hal, R. Kleppinger, J. A. J. M. Vekemans, R. A. J. Janssen and E. W. Meijer, *Chem. Mater.*, 2001, **13**, 2675; (c) G. Kestemont, V. de Halleux, M. Lehmann, D. A. Ivanov, M. Watson and Y. H. Geerts, *Chem. Commun.*, 2001, 2074; (d) J. Yin, H. Qu, K. Zhang, J. Luo, X. Zhang, C. Chi and J.-S. Wu, *Org. Lett.*, 2009, **11**, 3028.
- (a) B. A. Jones, A. Facchetti, M. R. Wasielewski and T. J. Marks, *J. Am. Chem. Soc.*, 2007, **129**, 15259; (b) B. A. Jones, A. Facchetti, T. J. Marks and M. R. Wasielewski, *Chem. Mater.*, 2007, **19**, 2703; (c) K. C. See, C. Landis, A. Sarjeant and H. E. Katz, *Chem. Mater.*, 2008, **20**, 3609.
- (a) Z. An, J. Yu, S. C. Jones, S. Barlow, S. Yoo, B. Domercq, P. Prins, L. D. A. Siebbeles, B. Kippelen and S. R. Marder, *Adv. Mater.*, 2005, **17**, 2580; (b) Y. Che, A. Datar, K. Balakrishnan and L. Zang, *J. Am. Chem. Soc.*, 2007, **129**, 7234.
- (a) J. Arient, *Russ. Chem. Rev.*, 1965, **34**, 826; (b) M. Herbst and K. Hunger, *Industrial Organic Pigments*, VCH, New York, 1993; (c) X. Li, Y. Xiao and X. Qian, *Org. Lett.*, 2008, **10**, 2885.
- R. P. Ortiz, H. Herrera, R. Blanco, H. Huang, A. Facchetti, T. J. Marks, Y. Zhang and J. L. Segura, *J. Am. Chem. Soc.*, 2010, **132**, 8440.
- The molecular geometry and energy levels were calculated using DFT/B3LYP/6-311G** with Q-Chem 3.2. Methyl groups were used as the side chain. See ESI† for more computational details.
- D. Z. Rogers, *J. Org. Chem.*, 1986, **51**, 3905.
- P. Ganesh, X. Yang, J. Loos, T. J. Savenije, R. D. Abellon, H. Zuilhof and E. J. R. Sudhoelter, *J. Am. Chem. Soc.*, 2005, **127**, 14530.
- The energy levels of the LUMO of these electroactive compounds are derived using the following equation: LUMO = $-(E_{\text{red}} + 4.8 \text{ eV})$ where E_{red} is the first reduction potential versus $E_{\text{F}}/E_{\text{F}}^+$. The redox potentials were determined as the midpoints between peak potentials for the forward and reverse scans. HOMO energies are deduced from the optical bandgap. See ref. 16.
- (a) Y. Che, X. Yang, G. Liu, C. Yu, H. Ji, J. Zuo, J. Zhao and L. Zang, *J. Am. Chem. Soc.*, 2010, **132**, 5743; (b) L. Zhang, Y. Che and J. S. Moore, *Acc. Chem. Res.*, 2008, **41**, 1596.